DOI: 10.1002/ejic.200900365

X-ray Structures, Spectroscopic and Magnetic Studies of a Coordination Polymer Series Based on a TTF Derivative and Paramagnetic Transition Metals

Jean Olivier,[a] Stéphane Golhen,*[a] Roman Świetlik,[b] Olivier Cador,[a] Fabrice Pointillart,[a] and Lahcène Ouahab*[a]

Keywords: Polymers / Magnetic properties / Cadmium / Cobalt / Manganese / Zinc

The oxidation of 2,3,6,7-tetrakis(2-cyanoethylthio)tetrathiafulvalene (TCE-TTF) with hexafluoroacetylacetonate (hfac) salts of paramagnetic (Co^{II}, Mn^{II}) and diamagnetic (Zn^{II}, Cd^{II}) ions in the presence of tetrahedral anions (BF_4^- and ClO_4^-) resulted in the isolation of four isostructural salts. The structure of these salts revealed an infinite two-dimensional network due to the coordination of the nitrilo arms of TCE-TTF to the metal. Short interplanar S···S interactions between two planes involving TCE-TTF give a third dimension to this polymer. TTF ligands are fully oxidized, and hence these materials show semiconducting behaviour. Spectroscopic and magnetic studies of the paramagnetic-transition-metal-containing polymers are also presented.

Introduction

The search for materials in which magnetism and electrical conductivity coexist is one of the main challenges in the field of multifunctional materials.[1] The tetrathiafulvalene (TTF) molecule and its derivatives are certainly the most popular units to build conducting and superconducting networks. The supramolecular architectures based on transition metals and organic building blocks are of great interest and great efforts have been made to synthesize new organic building blocks to improve the properties of the materials. Numerous TTF derivatives bearing *N*-coordinating groups were synthesized and linked to various ions such as transition-metal[2] or rare-earth ions.[3] Some of these extended TTF molecules are prepared by a phosphite-based coupling reaction from a 3,4-cyanoethylthio-1,3-dithiole-2-thione and a dithiole – one molecule.[4] The TTF tetrathiolate 2,3,6,7-tetrakis(2-cyanoethylthio)tetrathiafulvalene (TCE-TTF abbreviated as L hereafter) (Scheme 1) can be obtained from this reaction. In L the TTF skeleton is functionalized with four electron-withdrawing 2-cyanoethylthio groups, which are able to coordinate transition metals and to produce numerous new kinds of polymeric architectures.

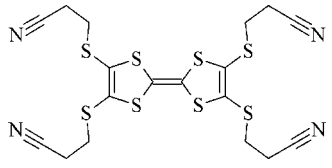

Scheme 1. TCE-TTF.

The TCE-TTF molecule is not so popular as a starting building block.[5] To the best of our knowledge, this TTF derivative was used as starting compound for radical salts[6] as well as for 3D silver organic frameworks.[7] In the following, we will present the synthesis, crystal structure, optical and magnetic characterizations of four isostructural homobimetallic materials involving the radical form of TCE-TTF. These compounds are formulated as $[M^{II}(TCE\text{-}TTF^{\cdot+})_2M^{II}(H_2O)_4](X)_6{\cdot}2H_2O$, X = BF_4^- for M = Co^{II} (Co-$L^{\cdot+}$) and X = ClO_4^- for M = Mn^{II} (Mn-$L^{\cdot+}$), Zn^{II}, (Zn-$L^{\cdot+}$), Cd^{II} for (Cd-$L^{\cdot+}$). The four arms of the TTF radical derivatives are coordinated to transition-metal ions to form a 2D polymeric network. Short S···S contacts between TTF cores of these 2D polymers complete the pseudo-3D architecture. Details of the crystal structures are discussed. These compounds revealed semiconducting behaviour, with a resistivity value about 4×10^4 Ωcm for Co-$L^{\cdot+}$. The magnetic

[a] UMR 6226 CNRS-Université de Rennes 1 "Sciences Chimiques de Rennes",
263 avenue Général Leclerc, CS 74205, 35042 Rennes cedex, France
Fax: +33-2-23236840
E-mail: stephane.golhen@univ-rennes1.fr
[b] Institute of Molecular Physics, Polish Academy of Sciences, ul. Mariana Smoluchowskiego 17, 60-179 Poznan, Poland
Supporting information for this article is available on the WWW under http://dx.doi.org/10.1002/ejic.200900365.

behaviour of Mn-L$^{\cdot+}$ and Zn-L$^{\cdot+}$ are discussed in relation with UV/Vis, infrared and Raman spectroscopic measurements of neutral TCE-TTF and the polymeric compounds.

Results and Discussion

Synthesis

TTF-based donor 2,3,7,8-tetrakis(2-cyanoethylthio)-tetrathiafulvalene (L) was synthesized by cross-coupling, with a procedure inspired by J. Becher.[8] The polymeric compounds were obtained by using the electrocrystallization technique with tetrabutylammonium salt in a benzene/tetrachloromethane/dichloromethane mixture (1:1:1) as electrolyte with L and M(hfac)$_2$·xH$_2$O in the anodic compartment of the cell. All compounds (M = Co^{II}, Mn^{II}, Zn^{II} and Cd^{II}) were obtained with the perchlorate salt, but only tetrafluoroborate salts yield single crystals suitable for X-ray diffraction for the cobalt compound.

Single-Crystal X-ray Diffraction Structures

All structures were refined from data collected at room temperature. Data for Mn-L$^{\cdot+}$ were collected only at 100 K, because of the low stability of the crystals at room temperature (see Tables 1 and 2). Co-L$^{\cdot+}$ as well as Zn-L$^{\cdot+}$ compounds were additionally studied at 100 K. Crystallographic data and refinement parameters are presented in Tables 3 and 4 for all compounds at different temperatures. Since all materials are isostructural, only the structure of Co-L$^{\cdot+}$ is described for data collected at 293 K and 100 K.

The materials crystallize in the $P2_1/c$ space group of the monoclinic system. The asymmetric unit consists of two metal ions, called M1 and M2 and located at two inversion centre sites (2d and 2a Wyckoff positions, respectively), one TCE-TTF, three BF_4^- anions and three water molecules. The unit cell contains four TCE-TTF donor molecules, four M^{II} metal ions, twelve monoanions and twelve water molecules. The stoichiometry of the salts as well as the central C3–C4 bond lengths prove that TTF molecules are oxidized in all compounds and carry an entire (+1) positive charge. TCE-TTF$^{\cdot+}$ molecules lie in general positions. An ORTEP plot of the asymmetric unit of compound Co-L$^{\cdot+}$ with the atomic numbering scheme is shown in Figure 1. The four nitrilo arms of the molecule lie on the same side of the plane formed by the S3–S4–C3–C4–S5–S6 atoms of the TTF skeleton. Each TCE-TTF$^{\cdot+}$ coordinates three different Co^{II} ions with the four different nitrogen atoms of the four nitrilo groups. On one side of the molecule, N3 and N4 are bonded to M1, while on the other side N1 and N2 are bonded to M2 and a-translated M1, respectively.

Table 1. Selected bond lengths in Å and angles in ° for compounds Co-L$^{\cdot+}$, Mn-L$^{\cdot+}$, Zn-L$^{\cdot+}$ and Cd-L$^{\cdot+}$.

	Co-L$^{\cdot+}$		Mn-L$^{\cdot+}$	Zn-L$^{\cdot+}$		Cd-L$^{\cdot+}$
	293 K	100 K	100 K	293 K	100 K	293 K
M1–N2^{iv}	2.110(4)	2.123(3)	2.251(4)	2.139(6)	2.163(2)	2.323(7)
M1–N3	2.106(4)	2.103(3)	2.207(4)	2.119(6)	2.115(2)	2.291(7)
M1–N4	2.122(4)	2.125(3)	2.241(4)	2.160(6)	2.163(2)	2.352(7)
M2–N1	2.099(4)	2.093(3)	2.197(4)	2.120(5)	2.101(2)	2.290(7)
M2–O1	2.071(3)	2.072(2)	2.172(3)	2.081(4)	2.0963(16)	2.268(5)
M2–O2	2.100(3)	2.106(2)	2.210(3)	2.132(4)	2.1242(16)	2.302(5)
C3–C4	1.383(5)	1.381(4)	1.379(6)	1.372(7)	1.392(3)	1.385(9)
C9–N1	1.131(5)	1.138(4)	1.137(5)	1.117(7)	1.146(3)	1.128(9)
C12–N2	1.128(6)	1.134(4)	1.143(6)	1.136(8)	1.138(3)	1.136(9)
C15–N3	1.139(5)	1.140(4)	1.138(6)	1.130(7)	1.136(3)	1.126(9)
C18–N4	1.143(6)	1.136(4)	1.140(6)	1.137(8)	1.142(3)	1.135(9)
N3–M1–N2^{iv}	85.71(15)	84.62(11)	83.93(14)	86.0(2)	84.55(8)	84.8(3)
N3–M1–N4	85.65(15)	85.48(11)	85.49(14)	86.6(2)	86.35(8)	85.0(2)
N2^{iv}–M1–N4	90.69(16)	90.90(11)	92.11(14)	91.1(2)	91.80(8)	91.7(3)
O1–M2–N1	85.94(13)	86.31(10)	86.67(13)	86.30(19)	86.37(7)	87.3(2)
O1–M2–O2	90.82(13)	90.16(9)	89.36(11)	90.94(18)	90.79(6)	90.9(2)
N1–M2–O2	90.85(15)	90.15(10)	90.51(12)	91.2(2)	90.29(7)	91.8(2)

Symmetry code iv: 1 + x, y, z.

Table 2. Intermolecular contacts in Å and mean plane angles in ° for compounds Co-L$^{\cdot+}$, Mn-L$^{\cdot+}$, Zn-L$^{\cdot+}$ and Cd-L$^{\cdot+}$.

	Co-L$^{\cdot+}$		Mn-L$^{\cdot+}$	Zn-L$^{\cdot+}$		Cd-L$^{\cdot+}$
	293 K	100 K	100 K	293 K	100 K	293 K
S4···S3^{xiv}	3.4230(14)	3.3125(11)	3.3674(14)	3.4833(19)	3.3642(8)	3.4833(24)
S4···S1^{xiv}	3.5526(15)	3.4731(12)	3.5120(14)	3.5765(22)	3.4968(8)	3.5877(26)
S7···S6^{xv}	3.5369(14)	3.4557(11)	3.5149(14)	3.5794(20)	3.5021(8)	3.5986(24)
S7···S8^{xv}	3.6640(15)	3.5999(12)	3.6173(14)	3.6612(21)	3.6181(8)	3.6571(26)
M1···M2	8.3094(1)	8.2350(6)	8.3382(8)	8.4054(1)	8.3428(4)	8.4264(5)
Angle D/D^{xv}	21.49(2)	21.97(2)	21.20(2)	20.18(3)	20.50(1)	20.12(3)

Symmetry codes xiv: 1 – x, –1/2 + y, 3/2 – z; xv: 2 – x, y + 1/2, 3/2 – z.

Table 3. Crystal data and structure refinement details for compounds based on paramagnetic metals Co-L$^{\cdot+}$ at 100 K and 293 K and Mn-L$^{\cdot+}$ at 100 K.

	Co-L$^{\cdot+}$		Mn-L$^{\cdot+}$
Temperature	100 K	293 K	100 K
Formula	$C_{36}H_{44}B_6Co_2F_{24}N_8O_6S_{16}$	$C_{36}H_{44}B_6Co_2F_{24}N_8O_6S_{16}$	$C_{36}H_{44}Cl_6Mn_2N_8O_{30}S_{16}$
Fw	1836.47	1836.47	1904.33
T /K	293(2)	100(2)	100(2)
Crystal system	monoclinic	monoclinic	monoclinic
Space group	$P2_1/c$	$P2_1/c$	$P2_1/c$
a /Å	12.9835(2)	12.9754(13)	13.0984(18)
b /Å	10.3738(2)	10.1439(9)	10.3215(12)
c /Å	26.8355(4)	26.480(3)	26.751(4)
β /°	103.024(1)	102.775(5)	102.452(7)
V /Å^3	3521.45(10)	3399.1(6)	3531.5(8)
Z	2	2	2
$\rho_{calcd.}$ /g cm^{-3}	1.732	1.794	1.791
μ /cm^{-1}	1.056	1.094	1.144
F(000)	1840	1840	1928
θ range /°	2.48/25.33	2.49/27.59	2.52/27.43
Index ranges	$-15 \le h \le 15$	$-16 \le h \le 16$	$-16 \le h \le 16$
	$-12 \le k \le 11$	$-11 \le k \le 13$	$-13 \le k \le 12$
	$-32 \le l \le 32$	$-34 \le l \le 34$	$-34 \le l \le 34$
Reflections collected	11658	30869	32604
Reflections unique	6425	7823	8038
R(int)	0.0243	0.0597	0.0768
Completeness to θ	99.8%	99.1%	99.7%
Data/restraints	6425/0	7823/0	8038/0
Parameters	501	445	445
Goodness on fit on F^2	1.027	1.028	1.122
R_1 [$I > 2\sigma(I)$][a]	0.0478	0.0429	0.0610
wR_2 [b]	0.1232	0.1050	0.1334
R_1 (all data)[a]	0.0657	0.0650	0.0754
wR_2[b]	0.1361	0.1174	0.1409
Largest diff. peak and hole /e$^-$ Å^{-3}	1.124, –0.940	1.504, –0.886	1.157, –0.726

[a] $R_1 = \Sigma||F_o| - |F_c||/\Sigma|F_o|$. [b] $wR_2 = \{\Sigma[w(F_o^2 - F_c^2)^2]/\Sigma[w(F_o^2)^2]\}$.

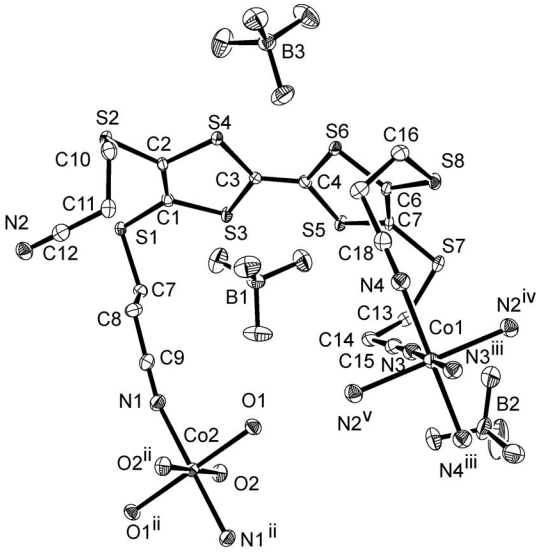

Figure 1. ORTEP (50% probability ellipsoids) structure of the asymmetric unit of Co-L$^{\cdot+}$ at 100 K, with labelling scheme and completed cobalt coordination spheres. Hydrogen atoms and non-coordinated water molecules are omitted for clarity. The symmetry codes are ii: $1-x, 2-y, 1-z$; iii: $2-x, 1-y, 1-z$; iv: $1+x, y, z$; v: $1-x, 1-y, 1-z$.

The centrosymmetric coordination spheres of the two metals ions M1 and M2 are different. That of M1 is built up with six nitrogen atoms from four TCE-TTF$^{\cdot+}$. The three independent M1–N bond lengths are almost identical at room temperature for all compounds (see Table 1). These bond length variations differ on lowering the temperature from 293 K to 100 K. While the Co1–N3 and Co1–N4 bond lengths remain constant [from 2.106(4) to 2.103(3) Å and from 2.122(4) to 2.125(3) Å, respectively] the Co1–N2 bond length surprisingly increases from 2.110(4) to 2.123(3) Å. One can notice that on cooling from room temperature the coordination sphere is compressed along the N3–M1–N3^{iii} axis. The second metal ion M2 lies in a centrosymmetric octahedral coordination sphere built with four oxygen atoms O1 and O2 from water molecules and two N1 nitrogen atoms belonging to two TCE-TTF$^{\cdot+}$.

As a result of both centrosymmetry and translation, the TCE-TTF$^{\cdot+}$ and M1 form infinite double TCE-TTF/M1 chains along the a axis (see Figure 2).

The second metal site M2 acts as a bridging unit between two double chains in the b direction to build a polymeric 2D network lying in the ab plane (see Figure 3). For Co-L$^{\cdot+}$ at 293 K, the shortest distance observed between metals Co1 and Co2 is equal to 8.3094(1) Å. All M1···M2 dis-

Table 4. Crystal data and structure refinement details for compounds based on diamagnetic metals Zn-$L^{\cdot+}$ at 100 K and 293 K and Cd-$L^{\cdot+}$ at 100 K.

	Zn-$L^{\cdot+}$		Cd-$L^{\cdot+}$
Temperature	100 K	293 K	100 K
Formula	$C_{36}H_{44}Cl_6N_8O_{30}S_{16}Zn_2$	$C_{36}H_{44}Cl_6N_8O_{30}S_{16}Zn_2$	$C_{36}H_{44}Cd_2Cl_6N_8O_{30}S_{16}$
Fw	1925.19	1925.19	2019.25
T /K	293(2)	100(2)	293(2)
Crystal system	monoclinic	monoclinic	monoclinic
Space group	$P2_1/c$	$P2_1/c$	$P2_1/c$
a /Å	13.1128(3)	13.0844(8)	13.158(1)
b /Å	10.5193(2)	10.3541(7)	10.530(1)
c /Å	26.7038(8)	26.4055(16)	27.248(1)
β /°	103.031(1)	102.454(3)	103.205(10)
V /Å^3	3588.60(15)	3493.2(4)	3675.5(5)
Z	2	2	2
$\rho_{calcd.}$ /g cm^{-3}	1.782	1.830	1.825
μ /cm^{-1}	1.442	1.481	1.334
F(000)	1948	1948	2020
θ range /°	2.47/28.70	2.53/27.42	2.45/27.49.
Index ranges	$-17 \le h \le 17$	$-16 \le h \le 16$	$-17 \le h \le 17$
	$-13 \le k \le 14$	$-12 \le k \le 13$	$-13 \le k \le 13$
	$-36 \le l \le 35$	$-34 \le l \le 34$	$-35 \le l \le 35$
Reflections collected	17337	37713	14987
Reflections unique	9241	7953	8416
R(int)	0.0880	0.0342	0.0509
Completeness to θ	99.7%	99.7%	99.9%
Data/restraints	9241/0	7953/0	8416/0
Parameters	445	445	445
Goodness on fit on F^2	0.932	0.794	0.985
R_1 [$I > 2\sigma(I)$][a]	0.0629	0.0291	0.0657
wR_2[b]	0.1542	0.0828	0.1767
R_1 (all data)[a]	0.1738	0.0372	0.1517
wR_2[b]	0.2031	0.0932	0.2367
Largest diff. peak and hole /e$^-$ Å^{-3}	0.970, –0.979	0.840, –0.538	1.600, –1.310

[a] $R_1 = \Sigma||F_o| - |F_c||/\Sigma|F_o|$. [b] $wR_2 = \{\Sigma[w(F_o^2 - F_c^2)^2]/\Sigma[w(F_o^2)^2]\}$.

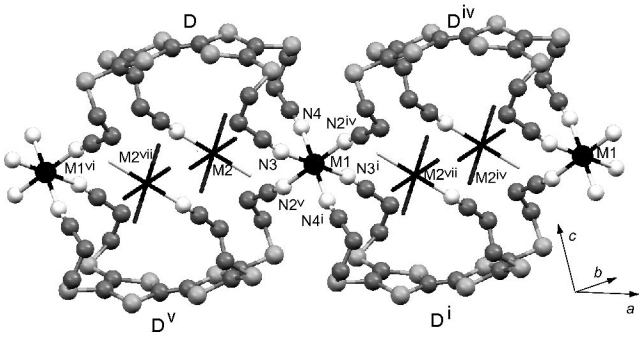

Figure 2. Double chain involving TCE-TTF and M1 ions along the a axis with symmetry codes i: $2 - x$, $1 - y$, $1 - z$; iv: $1 + x$, y, z; v: $1 - x$, $1 - y$, $1 - z$; vi: $-1 + x$, y, z; vii: x, $y - 1$, z; viii: $1 + x$, $1 - y$, z. BF_4^- ions and noncoordinated water molecules are omitted for clarity.

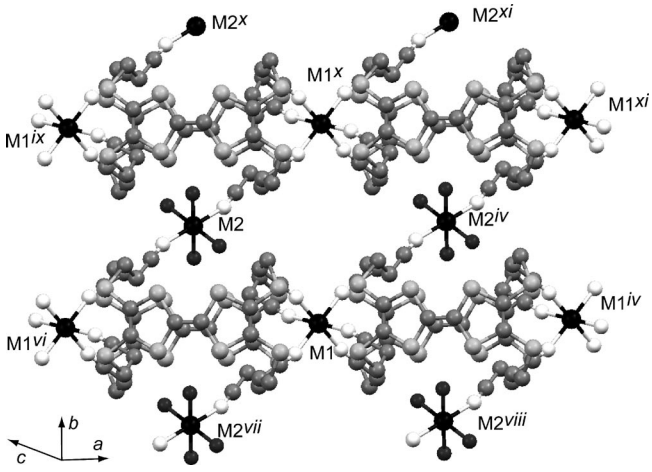

Figure 3. Double chains involving TCE-TTF and M1 ions along the a axis with symmetry codes i: $2 - x$, $1 - y$, $1 - z$; iv: $1 + x$, y, z; v: $1 - x$, $1 - y$, $1 - z$; vi: $-1 + x$, y, z; vii: x, $y - 1$, z; viii: $1 + x$, $1 - y$, z; ix: $-1 + x$, $1 + y$, z; x: x, $1 + y$, z; xi: $1 + x$, $1 + y$, z. BF_4^- ions and noncoordinated water molecules are omitted for clarity.

tances are given in Table 2. The shortest M1···M1 and M2···M2 distances correspond to the unit cell parameter a. The ratio between the distance M2···M1 and the a parameter is the same for all compounds regardless of the temperature. It varies between 0.641 and 0.633.

Two 2D polymeric networks are crystallographically related by 2_1 screw axes; the networks are packed along the c axis. Short S···S contacts are observed between these net-

works; at 293 K, for Co-L$^{\cdot+}$, the shortest S4···S3^{xiv} contact is equal to 3.4230(14) Å, which is much shorter than the sum of the van der Waals radii (2 × 1.80 Å = 3.6 Å).[9] The angle between the mean planes formed by the S3–S4–C3–C4–S5–S6 atoms of the TTF skeleton of two adjacent TCE-TTF$^{\cdot+}$ moieties belonging to two neighbouring 2D networks is equal to 21.49(2)°. All contacts shorter than double the van der Waals radius of sulfur atoms and the angle between the mean planes are given in Table 2. For all compounds, this angle increases as the temperature decreases, while the shortest S3···S4 intermolecular contact increases (Figure 4). All short distances involving anions and water molecules lie within one 2D polymeric network; nevertheless, one anion connects two networks as a result of C1···F11–B3–F9···C17 contacts that are shorter by about 0.02 to 0.04 Å than the sum of the van der Waals radii of the corresponding atoms.

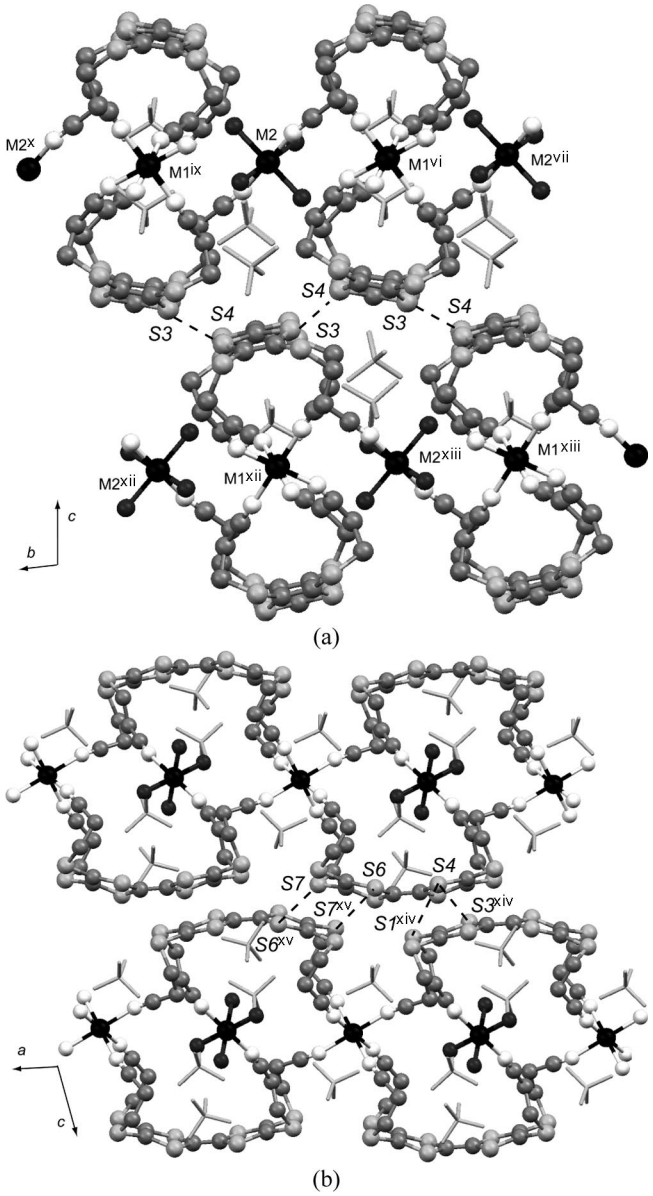

Figure 4. Interactions between two networks with shortest intermolecular S···S contacts listed in Table 2 (a) viewed along the *a* axis; (b) viewed along the *b* axis. The symmetry codes are vi: –1 + *x*, *y*, *z*; vii: *x*, *y* – 1, *z*; ix: –1 + *x*, 1 + *y*, *z*; x: *x*, 1 + *y*, *z*; xii: 1 – *x*, 1/2 + *y*, 1/2 – *z*; xiii: 1 – *x*, *y* – 1/2, 1/2 – *z*; xiv: 1 – *x*, –1/2 + *y*, 3/2 – *z*; xv: 2 – *x*, *y* + 1/2, 3/2 – *z*.

Magnetism

The temperature dependence of the magnetization of microcrystalline samples of Mn-L$^{\cdot+}$ and Zn-L$^{\cdot+}$ has been measured in the 2–300 K temperature range. The $\chi_M T$ vs. T plots, χ_M being the molar magnetic susceptibility and T the temperature in Kelvin, are represented in Figure S1. The value of $\chi_M T$ for Mn-L$^{\cdot+}$ is almost constant (Curie behaviour) and equal to approximately 8.6 cm^3 K mol^{-1}, which is much lower than the expected value (9.5 cm^3 K mol^{-1}) for four uncoupled spins: two 5/2 spins of two Mn^{II} ions (g_{Mn} = 2.00) and two 1/2 spins of two TCE-TTF$^{\cdot+}$ (g = 2.00). The experimental value is, however, close to the expected one for two uncoupled Mn^{II} spins (8.75 cm^3 K mol^{-1}). Zn-L$^{\cdot+}$ is nonmagnetic with a $\chi_M T$ value of approximately 0.06 cm^3 K mol^{-1}. It appears that the TCE-TTF$^{\cdot+}$ radical cations in both compounds do not contribute to the overall magnetism. Two hypotheses can then be formulated: (i) the TCE-TTF are not radical cations (ii) the TCE-TTF$^{\cdot+}$ radical cations are so strongly antiferromagnetically coupled that they do not contribute significantly, even at room temperature. At room temperature, the contribution of the radical network to the magnetism is equal to 8% of the expected contribution for uncoupled species (0.75 cm^3 K mol^{-1}). Therefore, one may say that the paramagnetism of Mn-L$^{\cdot+}$ arises almost entirely from the uncoupled spins at the metal sites. IR, Raman and UV/Vis absorption spectroscopy have been performed to validate one of the hypotheses.

IR and Raman Spectroscopy

The vibrational spectra of the polymeric compounds have to be discussed in comparison with the spectra of TTF[10]and other symmetrical TTF derivatives, e.g. TMTTF (tetramethyltetrathiafulvalene).[11] The most interesting spectral features of charge-transfer salts formed by TTF or its derivatives are normal modes related to the C=C stretching vibrations. The frequency of these modes strongly decreases when the average degree of ionization of the molecule grows. For this reason, the C=C modes of donor molecules were often studied by using IR and Raman spectroscopy in order to estimate the degree of ionization of molecules or its modifications as a result of charge ordering phenomena.[12] The C≡N stretching modes are other interesting spectral features, as the electron-withdrawing C≡N group is coordinated with metal atoms.

Neutral TCE-TTF crystallizes in the monoclinic space group $P2_1/n$;[5] there are two molecules per unit cell (Z = 2). The molecules have a planar structure with the exception of four cyanoethyl groups, which are arranged on opposite sides of the molecular plane. The IR absorption spectrum

of a single crystal of neutral L is shown in Figure S2. We observe two bands related to the C≡N stretching vibrations at 2231 and 2250 cm^{-1}. In the C=C stretching vibration region, a band at 1492 cm^{-1} is related to the antisymmetric stretching mode of C=C bonds of the ring (for neutral TMTTF this band has been observed at 1627 cm^{-1}).[11] In Raman spectra of neutral L, two bands related to symmetrical C=C stretching vibrations of the TTF are observed at 1555 and 1488 cm^{-1} (in neutral TMTTF these two bands are at 1639 and 1538 cm^{-1}, respectively[11]).

The single-crystal IR absorption spectra of Co-$L^{\cdot+}$ and Mn-$L^{\cdot+}$ at room temperature are displayed in Figure 5. The strong bands above 3000 cm^{-1} are attributed to water molecules, which are present in the crystals (O–H stretching). The strong band at 1642 cm^{-1} (Co-$L^{\cdot+}$) and 1645 cm^{-1} (Mn-$L^{\cdot+}$) can also be related to water bound in crystals (O–H deformation). These bands are sharp and well-reproducible for different samples, providing evidence that water molecules in crystals are well bound and ordered. In comparison with the neutral L, the C≡N bands are shifted at higher frequencies by about 50 cm^{-1}; i.e., all groups are coordinated. In both crystals a band at 1424 cm^{-1} is observed, which is assigned to the IR-active antisymmetric vibration of ring C=C bonds of TTF. As a result of the oxidation, this band is shifted by about 68 cm^{-1} (oxidation of TTF[10] or TMTTF[11] causes a shift of 52 or 80 cm^{-1}, respectively). The strong vibrational feature in the frequency region 900–1200 cm^{-1} consists of several strongly overlapping lines, and it should be related to C–H bending vibrations in the four cyanoethyl arms. In our compounds these arms are strongly bent and located in different crystallographic environments, and therefore, contrary to neutral L, we observe such a broad C–H bending feature.

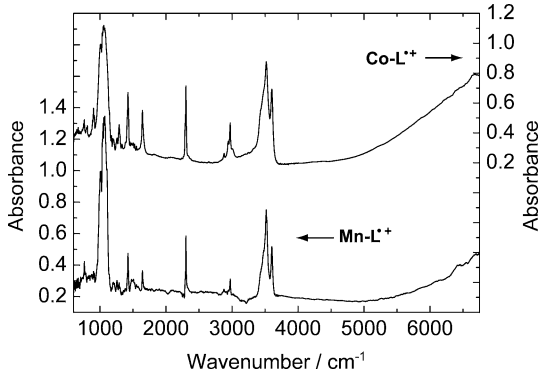

Figure 5. Infrared absorption spectra of single crystals of Co-$L^{\cdot+}$ and Mn-$L^{\cdot+}$.

As mentioned above, the most interesting are C=C stretching bands, which are clearly observed not only in IR spectra (Figure 5) but first of all in Raman spectra (Figure 6). In Figure 6 (bottom), we show the Raman spectrum of Co-$L^{\cdot+}$. Three C=C bands are observed: those at 1411 and 1454 cm^{-1} are assigned to Raman-active symmetrical vibrations of C=C bonds (analogous vibrations of TTF cations were found at 1420 and 1505 cm^{-1}, and at 1418 and 1567 cm^{-1} for TMTTF cations[11]). The third band at 1425 cm^{-1} is assigned to the antisymmetric dimeric mode of IR-active vibrations of TCE-$TTF^{\cdot+}$. The corresponding IR band related to antisymmetric C=C vibrations of the monomers is clearly observed in the IR spectrum (see above). When TTF derivatives in charge-transfer salts are strongly packed as dimers, the antisymmetric dimeric mode of antisymmetric monomer vibrations becomes Raman-active.[13] Normally, such a phenomenon is observed in Raman spectra of charge-transfer salts in the case of a strong charge-transfer interaction between monomers. In our case the charge transfer interaction between L molecules, if it exists, is probably weak; but, on the other hand, the molecules are connected through coordination bonds, and it seems to be

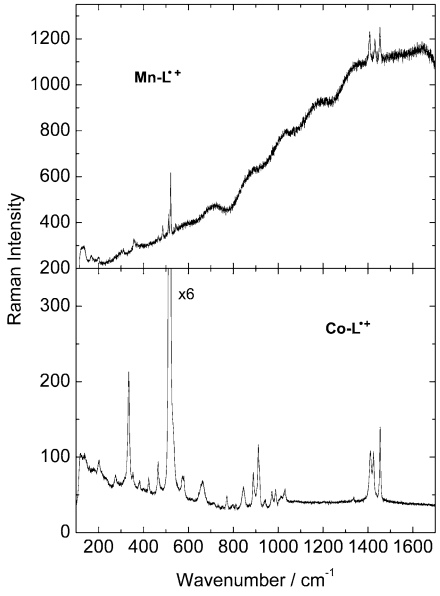

Figure 6. Raman spectra of Mn-$L^{\cdot+}$ (top) and Co-$L^{\cdot+}$ (bottom) single crystals measured with excitation at λ = 632.8 nm.

Table 5. Selected vibrational bands in wavenumbers of neutral TCE-TTF, Co-$L^{\cdot+}$ and Mn-$L^{\cdot+}$.

L		Co-$L^{\bullet+}$		Mn-$L^{\bullet+}$		Assignment
IR	Raman	IR	Raman	IR	Raman	
		3603		3603		H_2O
		3519		3517		
		3477		3475		
		3439		3436		
2250		2302	2299	2302		C≡N
2231		2288	2290	2288		stretching
		1645		1642		H_2O
	1555		1454		1453	C=C sym. stretching
1496		1424	1425	1424	1430	C=C antisym. stretching
	1488		1411		1407	C=C sym. stretch.
	493		518		521	ring
			515		521	breathing

possible that such coupling can be strong enough to yield Raman activity of the antisymmetric dimeric mode. Analogous C=C bands are observed in Figure 6 (top) for Mn-$L^{\cdot+}$ at 1407, 1430 and 1453 cm^{-1}. Unfortunately, in Raman spectra of Mn^{II}-based single crystals, a strong fluorescence is always observed for excitation at λ = 632.8 nm. However, the most important features are well-resolved. For both compounds, strong bands related to the Raman-active ring breathing modes of TCE-TTF at 515 and 518 cm^{-1} are observed; on oxidation, they are shifted to higher frequencies in agreement with frequency shifts observed in TTF or TMTTF cations. The most important vibrational bands are collected in Table 5.

UV/Vis Spectroscopy

The photophysical properties of L, Co-$L^{\cdot+}$ and Zn-$L^{\cdot+}$ are determined by solid-state UV/Vis absorption spectroscopy (Figure 7 and Figure S3). In the absorption spectrum of L, we observe three absorption bands centred at 20700, 24000 and 35500 cm^{-1}. The lowest-energy absorption bands are characteristic of monoelectronic HOMO-*m*→LUMO+*n* charge transfers (CTs), in which the HOMO-*m* is a TTF-donor-centred π orbital and the LUMO+*n* is a 2-cyanoethylthio-acceptor-centred π* orbital.[14] The HOMO-*m* represents an orbital with a lower energy than that of the HOMO, while the LUMO+*n* represents an orbital with a higher energy than that of the LUMO. The highest-energy transition (35500 cm^{-1}) corresponds mainly to intramolecular π–π* transitions of the 2-cyanoethylthio moieties. In the absorption spectrum of Co-$L^{\cdot+}$ (the values for Zn-$L^{\cdot+}$ are given in square brackets hereafter), we observe a band centred at 14000 [14100] cm^{-1}. By analogy with previous studies,[3,14] this band should be attributed to an intramolecular charge transfer of one electron from a SOMO-*p* localized on the 2-cyanoethylthio groups to the SOMO localized on the $TTF^{\cdot+}$ fragment. The SOMO-*p* orbital has a lower energy than that of the SOMO. The absorption band centred at 31300 [33200] cm^{-1} is attributed to the SOMO→LUMO transition of TCE-$TTF^{\cdot+}$. This latter transition is analogous to the HOMO→LUMO transition of TTF-TCE, which is not observed in the UV/Vis range (<12500 cm^{-1}). Both absorption bands attest that TCE-TTFs in our polymers are radical cations.

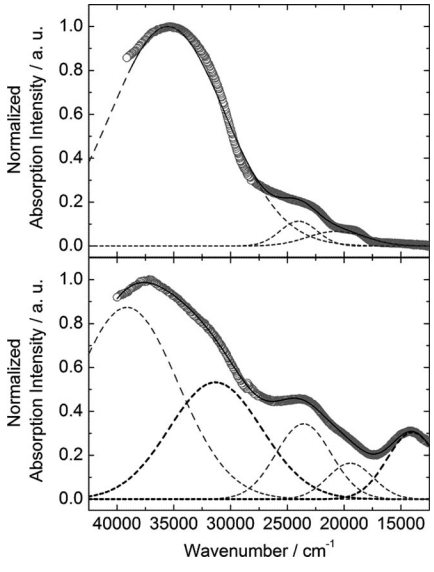

Figure 7. Experimental (open grey circles) solid-state UV/Vis absorption spectrum of L (top) and Co-$L^{\cdot+}$ (bottom), Gaussian deconvolution of the experimental curve (dashed lines) and the best fit (solid black lines) with R = 0.997 (for L) and R = 0.999 (for Co-$L^{\cdot+}$).

Conclusions

We have synthesized a series of polymeric compounds by using the electrocrystallization technique with the TCE-TTF donor, metal complexes and tetrahedral anions. The structures of the resulting materials have been determined by single-crystal X-ray diffraction. All compounds are isostructural; they consist of oxidized TTF derivatives covalently linked to a 3d transition metal as a result of a metal–nitrile interaction, which yields polymeric compounds. Magnetic measurements showed that TCE-$TTF^{\cdot+}$ do not contribute significantly to the overall magnetism, even at room temperature. IR/Raman and UV/Vis spectroscopic data provided clear evidence that the TCE-TTF molecules in the studied compounds are fully oxidized and strongly interact. These results have shown the ability of the tetra(alkylnitrile) TTF derivative to coordinate the metallic ion by means of its nitrogen atom. This opens the way to synthesize donors such as asymmetrical TTF derivatives bearing nitriles and *N*-coordinating groups to prepare heterometallic coordination architectures with magnetic and electronic behaviour.

Experimental Section

General: X-ray data were collected with an Enraf–Nonius four-circle diffractometer equipped with a CCD camera (CDFIX centre of Université de Rennes 1). The temperature dependence of the magnetization was recorded with a Quantum Design MPMS-XL SQUID magnetometer operating in the 2–300 K temperature range at a field of 1 T. The experimental data have been corrected for the diamagnetism of the sample holder and the intrinsic diamagnetism of the materials, as evaluated with use of Pascal's tables.

Synthesis

$M(hfac)_2{\cdot}2H_2O$:[15] The following general procedure was used to synthesize $M(hfac)_2{\cdot}2H_2O$ (where M = zinc and cadmium): in a test tube cooled to 0 °C, a solution of NH_4OH (25%, 0.67 mL, 6.22 mmol) was slowly added to H(hfac) (0.88 mL, 6.22 mmol). The aqueous phase was then extracted with ether (2 mL), and the organic fraction was poured into an aqueous solution of $M(NO_3)_2$ (3.11 mmol). After being stirred and settled, the organic phase was collected, and the aqueous phase was washed with another aliquot (2 mL) of ether. After the ether was removed from the organic fraction, $M(hfac)_2{\cdot}2H_2O$ was extracted from the resulting white powder by boiling in hexane for 30 min.

2,3,7,8-Tetrakis(2-cyanoethylthio)tetrathiafulvalene (TCE-TTF): 4,5-Bis(cyanoethylthio)-1,3-dithiol-2-thione (**1**, 2.50 mg, 8.22 mmol) was dissolved by a mixture of chloroform (75 mL) and acetic acid (25 mL). Mercuric acetate (6.30 g, 19.73 mmol) was then added. This solution was stirred overnight at room temp., filtered and washed two times with a saturated solution of $NaHCO_3$ and water. The solvent was partially removed before the addition of ethanol (200 mL), then the solution was cooled several hours at –20 °C. 4,5-bis(cyanoethylthio)-1,3-dithiol-2-one (**2**) was obtained as a white powder (2.05 g, yield 87%) and characterized by ^{1}H NMR ($CDCl_3$): δ = 3.18 (t, J = 7 Hz, 4 H); 2.83 (t, J = 7 Hz, 4 H) ppm.

Compounds **1** (1.24 g, 4.08 mmol) and **2** (783 mg, 2.72 mmol) were poured on dried toluene (100 mL), and freshly distilled triethylphosphite (10 mL) was added to the solution. After two hours of reflux at 120 °C, the mixture was slowly brought to room temp., the toluene was evaporated, and diethyl ether (150 mL) was added. After filtration and washing with diethyl ether (ca. 10 mL), colourful orange crystals of L were obtained with a yield of 78% (1.15 g). ^{1}H NMR ($CDCl_3$): δ = 3.18 (t, J = 7 Hz, 4 H); 2.83 (t, J = 7 Hz, 4 H) ppm.

Polymers: The electrocrystallization technique was used to produce these polymers. A solvent mixture (10 mL) of benzene/tetrachloromethane/dichloromethane (1:1:1) was added into each compartment of a U-shaped cell in which two compartments were separated by a glass frit. With much care, $[(C_4H_9)_4N]ClO_4$ (80 mg) was dissolved in each compartment, followed on the anode side by TCE-TTF (5 mg, 9×10^{-3} mmol) and $M(hfac)_2{\cdot}xH_2O$ (5×10^{-2} mmol, M = Co^{II}, Mn^{II}, Zn^{II} and Cd^{II}). Small black crystals appeared at the platinum anode shortly after a 0.5 μA constant current was applied. Suitable crystals for X-ray diffraction were obtained for Mn, Zn and Cd compounds, within two weeks. As only low-quality crystals were obtained with cobalt, the $[(C_4H_9)_4N]BF_4$ salt was used instead of the perchlorate.

X-ray Crystallography: Single crystals were mounted on a Nonius four-circle diffractometer equipped with a CCD camera and a graphite monochromated Mo-K_a radiation source (λ = 0.71073 Å), and data collection was performed at room temperature or at 100 K. Structures were solved by direct methods by using the programme SIR-97.[16] The refinement and all further calculations were carried out with SHELXL-97.[17] Hydrogen atom positions were calculated with a riding model. All non-hydrogen atoms were refined anisotropically, by using weighted full-matrix least-squares on F^2. Nor absorption correction, either one of the SQUEEZE processes was used (Table 3 and Table 4).

CCDC-727158, -727159, -727160, -727161, -727162, -727163 contain the supplementary crystallographic data for compounds Co-$L^{\cdot+}$ (at 293 and 100 K), Mn-$L^{\cdot+}$, Zn-$L^{\cdot+}$ (at 293 and 100 K) and Cd-$L^{\cdot+}$, respectively. These data can be obtained free of charge from The Cambridge Crystallographic Data Centre via www.ccdc.cam.ac.uk/data_request/cif.

Spectroscopy: UV/Vis absorption spectra were recorded by using the KBr disk method with a Varian Cary 5000 UV/Vis/NIR spectrometer equipped with a diffuse reflectance accessory sphere (Table 5). Room-temperature IR and Raman spectroscopic studies of single crystals of neutral L, Mn-$L^{\cdot+}$ and Co-$L^{\cdot+}$ were performed. The IR spectra were recorded by using a Bruker EQUINOX 55 FTIR spectrometer equipped with a Hyperion 1000 infrared microscope. The single-crystal Raman spectra were measured with a Raman spectrometer LABRAM HR800; the spectra were excited with a He-Ne laser (λ = 632.8 nm). The electrical vector of the laser beam was parallel to the direction corresponding to the maximum intensity of the Raman bands assigned to C=C stretching vibrations. The scattered light was collected in a backward-scattering geometry; the power of the laser beam was about 0.1 mW; the spectral resolution was 4 cm^{-1}.

Supporting Information (see footnote on the first page of this article): Temperature dependences of $\chi_M T$ for Mn-$L^{\cdot+}$ and Zn-$L^{\cdot+}$, the IR absorption spectrum of a single crystal of neutral TCE-TTF and the experimental solid state UV/Vis absorption spectrum of Zn-$L^{\cdot+}$ with its Gaussian deconvolution.

Acknowledgments

S. G. thanks Dr. M. Maesato (Kyoto University) for electrical measurements. This paper was partially supported by the Polish Ministry of Science and Higher Education as a research project in the years 2008–2010. We are indebted to Mr. S. Kamiński for help in spectroscopic measurements.

[1] a) T. Enoki, A. Miyazaki, *Chem. Rev.* **2004**, *104*, 5449–5478; b) E. Coronado, P. Day, *Chem. Rev.* **2004**, *104*, 5419–5448; c) L. Ouahab, T. Enoki, *Eur. J. Inorg. Chem.* **2004**, 933; d) H. Fujiwara, K. Wada, T. Hiraoka, T. Hayashi, T. Sugimoto, H. Nakazumi, K. Yokogawa, M. Teramura, S. Yasuzuka, K. Murata, T. Mori, *J. Am. Chem. Soc.* **2005**, *127*, 14166–14167; e) D. Lorcy, N. Bellec, M. Fourmigué, N. Avarvari, *Coord. Chem. Rev.* **2009**, *253*, 1398–1438.

[2] a) F. Iwahori, S. Golhen, L. Ouahab, R. Carlier, J.-P. Sutter, *Inorg. Chem.* **2001**, *40*, 6541–6542; b) C. Jia, S.-X. Liu, C. Ambrus, A. Neels, G. Labat, S. Decurtins, *Inorg. Chem.* **2006**, *45*, 3152–3154; c) L. Wang, B. Zhang, J. Zhang, *Inorg. Chem.* **2006**, *45*, 6860–6863; d) S. Ichikawa, S. Kimura, H. Mori, G. Yoshida, H. Tajima, *Inorg. Chem.* **2006**, *45*, 7575–7577; e) M. Chahma, N. Hassan, A. Alberola, H. Stoeckli-Evans, M. Pilkington, *Inorg. Chem.* **2007**, *46*, 3807–3809; f) E. Isomura, K.-i. Tokuyama, T. Nishinaga, M. Iyoda, *Tetrahedron Lett.* **2007**, *48*, 5895–5898; g) S. Ichikawa, S. Kimura, K. Takahashi, H. Mori, G. Yoshida, Y. Manabe, M. Matsuda, H. Tajima, J.-i. Yamaura, *Inorg. Chem.* **2008**, *47*, 4140–4145; h) F. Pointillart, Y. Le Gal, S. Golhen, O. Cador, L. Ouahab, *Inorg. Chem.* **2008**, *47*, 9730–9732.

[3] a) F. Pointillart, Y. Le Gal, S. Golhen, O. Cador, L. Ouahab, *Chem. Commun.* **2009**, 3777–3779; b) F. Pointillart, Y. Le Gal, S. Golhen, O. Cador, L. Ouahab, *Inorg. Chem.* **2009**, *48*, 4631–4633.

[4] L. Binet, J.-M. Fabre, C. Montginoul, K. B. Simonsen, J. Becher, *J. Chem. Soc. Perkin Trans. 1* **1996**, 783–788.

[5] G. Liu, G. Xue, W. Yu, W. Xu, Q. Fang, *Acta Crystallogr., Sect. E* **2002**, *58*, o842–o844.

[6] a) M. Tanaka, K. Shirasawa, J. Taka, S. Kashino, *Synth. Met.* **1999**, *103*, 2232–2233; b) J. Olivier, S. Golhen, O. Cador, L. Ouahab, *C. R. Chim.* **2008**, *11*, 673–683; c) E. W. Reinheimer, H. Zhao, K. R. Dunbar, *Synth. Met.* **2008**, *158*, 447–452.

[7] Y. Ding, Q. Chen, J.-C. Zhong, M. Munakata, H. Konaka, G.-L. Ning, H.-Z. Wang, *Polyhedron* **2008**, *27*, 1393–1400.

[8] N. Svenstrup, K. M. Rasmussen, T. K. Hansen, J. Becher, *Synthesis* **1994**, *8*, 809–812.

[9] A. Bondi, *J. Phys. Chem.* **1964**, *68*, 441–451.

[10] R. Bozio, I. Zanon, A. Girlando, C. Pecile, *J. Chem. Phys.* **1979**, *71*, 2282–2293.

[11] M. Meneghetti, R. Bozio, I. Zanon, C. Pecile, C. Ricotta, M. Zanetti, *J. Chem. Phys.* **1984**, *80*, 6210–6224.

[12] M. Dressel, N. Drichko, *Chem. Rev.* **2004**, *104*, 5689–5716.

[13] M. E. Kozlov, M. Tokumoto, *Synth. Met.* **1995**, *70*, 1023–1024.

[14] C. Jia, S.-X. Liu, C. Tanner, C. Leiggener, A. Neels, L. Sanguinet, E. Levillain, S. Leutwyler, A. Hauser, S. Decurtins, *Chem. Eur. J.* **2007**, *13*, 3804–3812.

[15] M. F. Richardson, W. F. Wagner, D. F. Sands, *J. Inorg. Nucl. Chem.* **1968**, *30*, 1275–1289.
[16] A. Altomare, M. C. Burla, M. Camalli, G. L. Cascarano, C. Giacovazzo, A. Guagliardi, A. G. G. Moliterni, G. Polidori, R. Spagna, *J. Appl. Crystallogr.* **1999**, *32*, 115–119.
[17] G. M. Sheldrick, *SHELXL97*, *Programs for Crystal Structure Analysis (Release 97–2)*, Institut für Anorganische Chemie der Universität Göttingen, Tammanstrasse 4, 3400 Göttingen, Germany, **1998**.

Received: April 21, 2009
Published Online: July 1, 2009

